ISSN: 0975-833X

Available online at http://www.journalcra.com

INTERNATIONAL JOURNAL OF CURRENT RESEARCH

International Journal of Current Research
Vol. 13, Issue, 10, pp.19306-19315, October, 2021

DOI: https://doi.org/10.24941/ijcr.42361.10.2021

RESEARCH ARTICLE

MANGANESE NANOMATERIALS AS DELIVERY SYSTEM IN COMBATING DISEASES

[1,*]Ardhendu Kumar Mandal and [2]Anindita Joardar

[1]Central Instrumentation Division, CSIR-Indian Institute of Chemical Biology, Kolkata, India,
[2]Department of Neurogenetics, Bangur Institute of Neurosciences, IPGME and R, Kolkata, India

ARTICLE INFO

Article History:
Received 17th July, 2021
Received in revised form
20th August, 2021
Accepted 14th September, 2021
Published online 30th October, 2021

Key Words:

Diseases; Manganese Nanomaterials; Synthesis and Functionalization; Mechanism ofaction; Biodistribution and Elimination; Therapeutic Efficacies.

[*]Corresponding author:
Ardhendu Kumar Mandal

ABSTRACT

Compromised immune individuals are chiefly affected by transmitted infectious agents or toxicants reflected by the annual demise of over 17 million globally. The conventional chemotherapy suffers from its high-dose requirements, poor bioavailability, low therapeutic indices, adverse side effects, development of multi-drug resistance, disability of crossing the biological barriers, and non-specific targeting. To overcome all the barriers, nanotechnology-based drug delivery systems have attracted attention as probable nanomedicine for the treatment of diseases. Manganese nanomaterials (MnNMs) such as manganese, manganese oxides and phosphate nanoparticles have gained interest owing to their suitable nanosize structures, easy surface modifications capability, cargos-vectoring ability, oxidative and non-oxidative microbicidal and anti-carcinogenic activities, photothermal effectivity and easy membrane penetrating ability to damage the cells. This review illustrates the recent advances regarding their synthesis, functionalization, mechanism of action, therapeutic efficacies, toxicity, biodistribution, pharmacokinetics and elimination for the application in targeted delivery as potential therapeutics against infectious diseases and cancer.

Citation: Ardhendu Kumar Mandal and Anindita Joardar. *"*Manganese nanomaterials as delivery system in combating diseases*", 2021. International Journal of Current Research, 13, (10), 19306-19315.*

INTRODUCTION

Emerging infectious diseases and cancer including brain tumor are caused by the administration of microbes and toxicants. Generally, the human antioxidant defense system and innate and acquired immune system have the capability to protect the body from the infection and disease -initiation (Mandal, 2021). However, toxicants, contagious and virulent agents, or microorganisms are transmitted into the host body overpowering body defense mechanisms to initiate site-infections by their multiplications and / or intra and extra -cellular host cells -injuries in the body resulting in tissue damage (National Institutes of Health (US), 2007). Tumor cells acquire resistance by increasing the intracellular glutathione (GSH) levels to neutralize intracellular reactive oxygen species (ROS) through hydrogen donation, and proliferate rapidly in the distorted tumor vasculatures due to the insufficient oxygen supply in tumor microenvironment by activating the hypoxia inducible factor (HIF) linked to cell proliferative signals (Bump and Brown, 1990; Brown, 2007; Muz *et al*., 2015; Teicher, 1995; Vaupel and Mayer, 2007; Rapisarda and Melillo, 2010).

The treatment of these diseases is hampered by drug for occurring drug resistance from re-emerging diseases, as well as for its non-specificity, toxicity, insolubility, non bio-accessibility to cells owing to biological barriers and non-specific targeting capability. To overcome these barriers, nanotechnology based metallic manganese nanoparticles have been developed as therapeutic agents for the treatment of infections and cancer. Manganese (Mn) and its oxidized chemical forms (MnO_2 or Mn_3O_4), the abundant transition element on the earth, have an important implication as micronutrient to maintain the proper growths, developments and functions of living organisms. As a cofactor, it activates many enzymes such as superoxide dismutase, galactosyl transferase, arginase, agmatinase, pyruvate carboxylase and glutamine synthetase for proper development of bones, cell structures, metabolism, mitochondrial antioxidant system and cell mortality (Avila *et al*., 2013; Schrantz *et al*., 1999). The nanoscale's materials have a large surface area to volume proportion which enhances not only their unique physical and chemical characteristics such as drug-absorption, reactivity with biological molecules, strength, sensitivity and stability including catalytic, electronic, optical, magnetic and

antimicrobial activities but also their penetrating features across the biological barriers (Born *et al*., 2006; Hoseinpour and Ghaemi, 2018; Jalal *et al*., 2010; Krolikowska *et al*., 2003; Zhao and Stevens, 1998; DeJong and Borm, 2008; Greish, 2010). As the materials, at the nanoscale level, can permeate into the cells creating membrane injury and generating reactive oxygen species (ROS), the cells or tissue may be damaged effectively (Apperlot *et al*., 2009; Shankar *et al*., 2009). In this context, nanomaterials may be easily functionalized on their surface with various ligands to get significant changes in their specific properties according to their needed biological applications. The cargos may be attached by conjugating selected ligands, sugars, proteins and antibodies for selected binding activity to specific target cells to improve their targeted drug delivery abilities and therapeutic efficacies at the pathological site/s (Mody *et al*., 2010). Conjugation of cargos, proteins, sugars and antibodies onto the surface of metal nanoparticles, protect them from the body's immune system extending their blood circulation time and thus their proper accumulation at the specific site/s of interest. Moreover, metal nanoparticles possess unique physico-chemical surface charges which enable them to act as potential therapeutics for the treatment of infections and diseased cells. Metallic nanomaterials, with or without ligand binding, accumulate actively to tumor cells via over-expressed antigens and through the enhanced permeability and retention (EPR) effect, or traverse through the enlarged pores in the capillary endothelium of the tumors passively (Maeda *et al*., 2000; Koo *et al*. 2011; Sudimack and Lee, 2000; Zhang *et al*., 2002; Mandal *et al*., 2014). In this concern, manganese dioxide nanoparticles (MnO_2 NPs) can catalyze hydrogen peroxide (H_2O_2) to water (H_2O) and molecular oxygen (O_2) to reduce tumor hypoxia as a crucial mediator (Zhu *et al*., 2016; Yang *et al*., 2017). Furthermore, manganese nanomaterials loaded with cargos may be anchored or coated on surface with biocompatible polymers such as poly (ethylene glycol) (PEG) phospholipid, poly (lactide-co-glycolide) (PLGA), polyvinyl pyrrolidone, polyacrylic acid, and salicylalchitosan to prevent the degradation of drugs in the process of delivery with a controlled manner of cytotoxic drug release to the disease zone/s with adequate dosage without harming healthy tissue (Na *et al*., 2007; Cho *et al*., 2017; Haneefa *et al*., 2017; Sana *et al*., 2017). This review focuses on the manganese nanomaterials as potential delivery system for the treatment of infectious diseases and cancer, based on their biological efficiencies.

Synthesis of manganese nanomaterials

Synthesis of manganese nanoparticles

Few methods of synthesis of Mn NMs-composites are described below:

The MnNPs may be synthesized utilizing air-free glovebox and Schlenk techniques. In this synthesis, 260 µL of oleic acid and 50 mg of $MnCl_2$ are mixed in an argon glovebox and added to 10 mL of diphenyl ether in a three-necked round-bottom Schlenk flask fitted with a rubber septum, thermometer adapter and condenser. In another Schlenk flask, 5 mL of diphenyl ether is mixed with 3 mL of 1.6 M n-butyl lithium (n-BuLi) in hexanes, and capped with a rubber septum. In this context, n-BuLi acts as a reductant to reduce Mn^{2+} to zerovalent Mn in a diphenyl ether solution, while oleic acid sticks to a thin amorphous oxide shell to coat the α-MnNPs for getting air-stability. After preparation, both the flasks are removed from the glovebox to connect to a Schlenk line under highly pure argon. After that, the metallic salt solution is warmed up to 200°C, and the n-BuLi solution is inoculated before removing the hexane from the n-BuLi solution by vacuum for the prevention from the over-pressure during injection. The solution turns to black from a blue-gray color instantly, followed by stirring for 20 min and then removal from the hotness. All the workups and the yield separation procedures are accomplished in the glovebox. The MnNPs may also be synthesized in another way. A freshly prepared aqueous solution (10 mL) of manganese acetate (1 mM) is admixed with pure lemon extract (10 mL) in a beaker and stirred for the reduction of manganese ions at 50-60 °C for 1 h to get pale yellow color from pale green. The freshly prepared curcumin extract (1 mM) may be added to the above solution to stabilize the nanoparticle with stirring for an additional 1 h. The change in color from yellow to yellowish brown and finally to reddish brown indicates the complete stabilization of MnNPs. pH between 3 and 4, temperature at 50-60 °C, and double distilled water are maintained and used throughout the experimental reaction. The solution is spun several times with washing to get pure MnNPs, while supernatant is decanted and kept in oven for drying.

For the synthesis of MnNPs, 2g air dried plant extracted powder is boiled with 30 mL sterile distilled water in a 100 mL Erlenmeyer flask for 2 min. After boiling, the solution mixture is filtered through the Whatmann no.1 filter paper. Then 5 mL of plant extract is adjoined to 25 mL of 1 mM potassium permanganate ($KMnO_4$) solution. The λ max at various time intervals are taken of the red color formed solution for 8 h utilizing UV-Visible spectroscopy. The solution is kept at room temperature for 24 h to settle nanoparticles completely. After that, the reaction mixture is spun and the supernatant is discarded. The pellet is suspended with 1 mL distilled water and cleansed by centrifugation. The pellet is collected by using alcohol / acetone / ethylacetate, dried, and stored as nanoparticles.

Synthesis of manganese oxide nanoparticles: 8g of dried powder of leaf extract is boiled with 200 mL of distilled water in an Erlenmeyer flask. The solution is cooled and spun at 3500 rpm for 15 min. The floating is collected in a colored bottle to store at 4°C. For the synthesis of MnO_2 NPs, various ratios (10, 25, and 50 %) of leaf extort and the aquatic solution of 0.01 mM manganese acetate [$(CH_3COO)_2$ $Mn.6H_2O$] at various pH (4, 6 and 8) are put together and stirred at room temperature for different time (40, 80 and 120 min). The deposits are collected by spinning of each sample with washing utilizing ethanol and distilled water several times, and then suspended in 7 mL of distilled water for the analysis to characterize them. For the synthesis of MnO_2 NPs in another way, 1:1 ratio of 1 M MnO_2 and the plant flower extract are mixed in a flask, and stirred at 100 rpm for 4 h. The resultant nanoparticles are purified by washing after spinning at 10000g for 20 min through the collection of pellets. The pellets are then freeze-dried and stored at -80◦C for further characterizations. MnO_2 NPs may also be synthesized by co-precipitation method utilizing two different anions of manganese salts (manganese II sulphate and oxalate). 0.2 M of both equal concentrated salts are admixed and stirred at 60°C to maintain the pH at 12 by adding NaOH solution, and continued stirring for 1 h at 60°C. The formed brown precipitate is filtered and cleansed with ethanol.

The precipitate is dried at 100°C for overnight, and then kept in muffle furnace at 500°C for 4 h.

Surface functionalizations of manganese nanomaterials: 1 mM of the salicylalchitosan (SC) is dissolved in ethanolic acetic acid mixture completely on a hot magnetic stirrer for 1 h. 1 mM of synthesized manganese nanomaterials are mixed slowly to the hot solution, and continued hot stirring for 2-3 h. The color changes from the dark brown to slow appearance of pale brown denote their functionalization. The reaction mixture is spun, cleansed several times with double distilled water and ethanol, and dried for further analysis. MnO_2 NPs are stabilized and functionalized with biocompatible polymers such as polyvinylpyrrolidone (PVP) and polyacrylic acid (PAA). In this functionalization, 31.5 mg $KMnO_4$ is liquefied in 9 mL of deionized (DI) water followed by stirring at 25°C for 30 min, and adding of 1 mL of PVP solution (37.4 mg / mL DI water). After 15 min, the same amount of PAA like PVP solution is adjoined to the reaction mixture. The change of color-solution from violet to wine takes place within 2 min. The stirring is continued at 25°C for an additional 15 min. The larger precipitates are removed by spinning at 5000 rpm. The supernatant is dialyzed for 60 h for removing unreacted free polymers and $KMnO_4$, and then freeze-dried for obtaining a brown powder of nanoparticles.

Characterisation of manganese nanocomposites: The formation, stability and biofunctionalization of manganese nanomaterials are determined by UV-Visible spectroscopy. The Mn contents in MnO_2 NPs are analyzed by inductive coupled plasma mass spectroscopy. The morphology of manganese nanocomposite materials is determined by transmission electron microscopy and scanning electron microscopy. The crystallinity of the synthesized MnO_2 NPs is detected by X-ray diffractometry. The purity and the nature of the synthesized MnO_2 NPs and functionalized NPs are detected by Fourier transform infrared spectroscopy. The hydrodynamic size and zeta potential of the MnO_2 NPs are determined by dynamic light scattering. The element mappings of MnO_2 NPs are detected by energy dispersive X-ray spectroscopy.

Mechanisms of action of manganese nanomaterials: The mechanistic actions of MnNMs imply to the generation of free metal ions -toxicity from the dissolution of nanoparticles-surfaces, oxidative stress owing to the production of ROS on nanopaticles-surfaces, and non-oxidative mechanisms for their metallic physico-chemical characteristics (Mandal, 2017; Mandal, 2017a; Mandal, 2018; Mandal, 2018a; Mandal, 2019; Aderibigbe, 2017; Sirelkhalim *et al*., 2015; Hajipur *et al*., 2012; Baker *et al*., 2005; Dizaj *et al*., 2014; Zong and Wang, 2014) (Figure 1 & Figure 2).

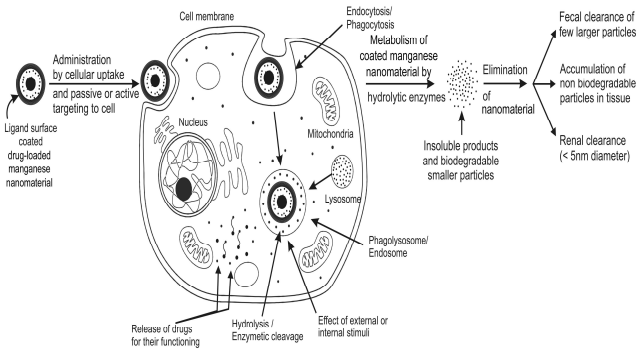

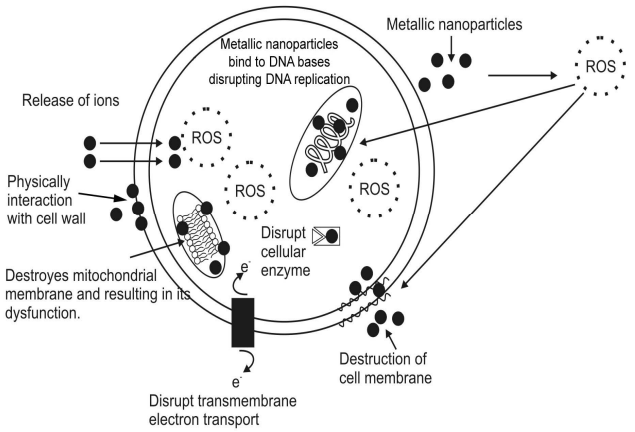

Fig. 1. Mode of action of metallic nanoparticles on cell

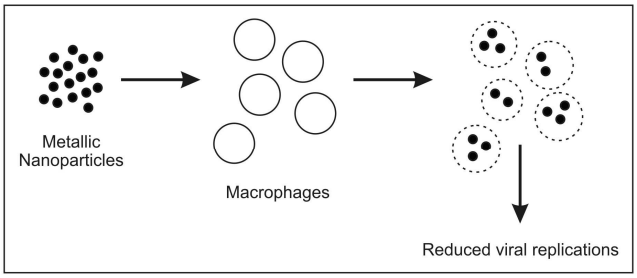

Fig.2. Mode of action of metallic nanoparticles on macrophages

The release of manganese ions or generation of ROS on the nanoparticles-surfaces may disrupt the cell walls by interaction or penetration the cell membranes, damage or modify membrane potential, inhibit CD4 dependent virion binding, block attachments, inhibit receptor binding sites, inhibit t-RNA binding to ribosome, decrease ATP level, leak intracellular contents, hamper cell differentiation, damage vital enzymes leading to the death of microbial or cancerous cells. Owing to the larger surface to volume ratio and nanosizes, the MnNMs can cross the membrane barriers and may be absorbed into the blood stream (Singh *et al*., 2011). Characteristically, tumor microenvironment displays mild acidity, GSH/H_2O_2 overproduction and hypoxia (Dai *et al*., 2017; Liu *et al*., 2018). To overcome these barriers, stable manganese oxides nanoparticles (MnOs NPs) have been designed for acting against tumor microenvironment. Firstly, all MnOs NPs can exhibit acid-responsive behaviors as transition metal oxides. Secondly, they can show activities of catalase (CAT) to catalyze H^+/H_2O_2 into oxygen (O_2) and Mn^{2+} (equations 1-5) (National Institutes of Health (US), 2007; Bump and Brown, 1990; Brown, 2007; Muz *et al*., 2015; Teicher, 1995) . Thirdly, oxidizing MnOs NPs can mimick glutathione peroxidase (GPx) for oxidizing GSH to GSSG (equations 6-9) (Vaupel and Mayer, 2007; Rapisarda and Melillo, 2010; Avila *et al*., 2013; Schrantz *et al*., 1999). The generated Mn^{2+} can catalyze H_2O_2 to produce hydroxyl radical ($^{\cdot}OH$) and Mn^{3+} by Fenton-like reactions (equation 10) (Born *et al*., 2006), and the resultant Mn^{3+} can catalyze H_2O_2 for producing superoxide anion ($^{\cdot}O_2^-$) and Mn^{2+} (equation 11) (Hoseinpour and Ghaemi, 2018) to destroy microbes and diseased cells.

$$MnO_2 + H_2O_2 + 2H^+ \rightarrow Mn^{2+} + 2H_2O + O_2 \quad 1$$
$$MnO + 2H_2O_2 + 2H^+ \rightarrow Mn^{2+} + 3H_2O + O_2 \quad 2$$
$$Mn_2O_3 + H_2O_2 + 4H^+ \rightarrow 2Mn^{2+}\ 3H_2O + O_2 \quad 3$$
$$Mn_3O_4 + H_2O_2 + 6H^+ \rightarrow 3Mn^{2+} + 4H_2O + O_2 \quad 4$$
$$MnO_x + H_2O_2 + 2H^+ \rightarrow Mn^{2+} + 2H_2O + X / 2O_2 \quad 5$$
$$MnO_2 + 2GSH + 2H^+ \rightarrow Mn^{2+} + GSSG + 2H_2O \quad 6$$
$$Mn_2O_3 + GSH + H^+ \rightarrow Mn^{2+} + GSSG + H_2O \quad 7$$
$$Mn_3O_4 + GSH + H^+ \rightarrow Mn^{2+} + GSSG + H_2O \quad 8$$
$$MnO_x + GSH + H^+ \rightarrow Mn^{2+} + GSSG + H_2O \quad 9$$

$Mn^{2+} + H_2O_2 \rightarrow Mn^{3+} + {}^{\cdot}OH + OH$ 10

$Mn^{3+} + H_2O_2 + OH^- \rightarrow Mn^{2+} + {}^{\cdot}O_2^- + 2H_2O$ 11

Moreover, manganese dioxide nanoparticles may act as non-invasive photodynamic therapeutics, owing to their excellent metallic physico-chemical features for the treatments of diseases, in which the excited photosensitizer can undergo type I electron transfer or type II energy transfer reactions to generate ROS resulting in necrosis or apoptosis of diseased cells (Gao *et al*., 2017; Aderibigbe, 2017).

The rapeutic applications of manganese nanomaterials: Manganese nanomaterials have been served as therapeutic agents for antimicrobial activity, chemotherapy, gene therapy, peptide / antibody therapy, immunotherapy, magnetic hyperthermia, starvation therapy, photodynamic therapy (PDT), chemodynamic therapy (CDT), sonodynamic therapy (SDT), photothermal therapy (PTT), radiotherapy (RT) and different combination therapy.

Antimicrobial activity: The various functionalized and non-functionalized manganese and manganese NPs have shown their antibacterial and antifungal activities against different bacterial and fungal strains through exhibiting various diameters of inhibition zone using agar well diffusion method (Cherian *et al*., 2016; Haneefa *et al*., 2017; Haneefa *et al*., 2017a; Jayandran *et al*., 2015). Their suitable characteristics such as nanosizes, different shapes with high surface area, adsorption, high chemical reactivity and charge have enabled them to interact efficiently with the biological systems to cause effective antimicrobial suppression (Wang *et al*., 2017). Biofilm formation due to antibiotic resistance in bacteria and their swimming motility ability have been reduced by MnO_2 NPs observed in soft agar medium (Ogunyemi *et al*., 2019; Mandal, 2018a). The transmission electron microscope study correlates the disruption in the morphology of the cell through its penetration by metallic NPs resulting in damage of the cell membrane and leakage of cell contents, while flow cytometry study relates the internalization of the NPs in live bacteria resulting in cell injury and ultimately apoptotic / necrotic cell death (Ogunyemi *et al*., 2019).

Chemotherapy: Manganese oxide NPs have been utilized to enhance chemotherapeutic drug delivery on the basis of TME-responsive drug release, circumventing multidrug resistance (MDR) and autophagy induction. For selective and controlled drug delivery into TME-site, pH, GSH and H_2O_2 -responsive DOX-loaded manganese oxide NMs are generally used to get their higher therapeutic efficacies evidenced by the high accumulation of drug within cancer cells through intracellular drug release (Chen *et al*., 2014; He *et al*., 2015; Ren *et al*., 2018). To overcome circumventing MDR, while P-glycoprotein (P-gp), the membrane bound ATR-binding cassette transporter encoded by MDR1, capable to pump free drug from the cytoplasm out of the cancer cell, drug-loaded manganese oxide NMs or their composites as chemotherapeutics have been applied to decrease the over-expression of P-gp by delivering more drug inside the cell and to decrease tumor hypoxia by generating O_2 and reducing the over-expression of HIF-1 (Yu *et al*., 2018; Thomas and Coley, 2003; Meng *et al*., 2010; Du *et al*., 2019; Zhang *et al*., 2017). Autophagy, the lysosome-dependent catabolic cellular salvage pathway to degrade biological macromolecules or a portion of abnormal organelles for reducing self-damage and maintaining the cellular homeostasis, is also responsible to induce cell death directly in its excessive or aberrant state (Li *et al*., 2009). DOX-loaded manganese oxide NPs can enhance chemotherapeutic efficiencies of drug by inducing autophagic cancer cell death forming autophagosome (Lu *et al*., 2013). DOX-loaded, oleic acid-coated hollow manganese oxide NPs, composite NMs such as UC NPs@$mSiO_2$-DOX-MnO_2, Fe_3O_4@SiO_2/$NaYF_4$-DOX-MnO_2, with or without coated PEG, have been applied to TME-site where MnO_2 is reduced to Mn^{2+} ions by GSH and drug is effectively released, and / or the tumor hypoxia is alleviated by simultaneous endogenous H_2O_2 degradation and glutathione reduction (Shin *et al*., 2009; Zhao *et al*., 2018; Zhao *et al*., 2014; Hao *et al*., 2013; Xu *et al*., 2018).

Gene therapy: Manganese oxide NMs such as MnO_2, hMn_3O_4 NPs have been used as enhanced gene delivery against various diseases for siRNA delivery and DNAzyme release (Du *et al*., 2019; Dunbar *et al*., 2018; Wang *et al*., 2019a). In MnO_2-DNAzyme nanosystem, the Mn^{2+} ions produced from degraded MnO_2, employed as cofactors of DNAzyme, facilitate gene-silencing therapy leading to death of cancer cells and anti-proliferation (Fan *et al*., 2015). In addition, siRNA and herceptin -loaded hollow MnO NPs coupled with 3,4-dihydroxy-L-phenylalanine and polyethylenimine have been utilized to target HER2 over-expressed cells for silencing of the target gene (Bae *et al*., 2011). Moreover, Ce_6DNAzyme-MnO_2 nanosystem has also been used for cancer therapy as effective photosensitized gene silencing application (Fan *et al*., 2015).

Peptide / antibody therapy: Doxorubicin loaded hollow manganese phosphate NPs have been functionalized with folic acid (FA) to treat cancer cells through folate receptor mediated endocytic targeting and drug release (Yoo and Park, 2004; Guo *et al*., 2011). MnO NPs have been coupled with antibody herceptin to target human epidermal growth factor receptor 2 (HER2) for homing to the tumor sites (Na *et al*., 2007; McCarthy and Weissleder, 2008). Herceptin loaded hollow MnO NPs coupled with 3,4-dihydroxy-L-phenylalanine and polyethylenimine have also been utilized to target HER2 over-expressed cells selectively for reducing tumor (Bae *et al*., 2011).

Immunotherapy: Immunotherapy is a strategy to activate the immune system and to enhance its innate power against diseases (Gopalakrishnan *et al*., 2018). Manganese oxide NPs have been used to serve as supporters and / or promoters for immunotherapy owing to their TME-responsive capabilities (Deng *et al*., 2018; Chu *et al*., 2019). MnO_2 NMs have been designed to integrate DOX and cytosine-phosphate-guanine (CpG)-Ag NPs for TME-mediated CpG and DOX deliveries (Wang *et al*., 2017a). Au@MnO_2 NPs have been utilized for image-guided O_2-boosted anti-tumor immunotherapy (Liang *et al*., 2018). In this context, the tumor-associated antigen produced from dying tumor cell may induce exposure and liberation of damage-associated molecular patterns (DAMPs) such as high mobility group protein B1 (HMGB1), ATP and calreticulin (CRT). The DAMPs, inturn, may induce the maturation of dendritic cells (DCs) to promote the activation of CD4 T cells, CD8 T cells and natural killer cells for the elimination of the primary tumor and the generation of the abscopal effect for the inhibition of metastases. PEG-modified Ce6 and DOX -loaded hollow MnO_2 NPs have also been utilized to serve as an oxygen generator for regulating polarization of tumor-associated macrophages (TAM) to

overcome tumor hypoxia by converting immunosuppressive M2 type TAM cells into reverse immunosuppressive M1 type TAM cells and activating immune responses through alterations of M2 macrophages-secreted interleukin-10 (IL-10) and M1 macrophages-secreted interleukin-12 (IL-12) (Yang *et al*., 2017; Pardoll, 2012; Facciabene *et al*., 2011).

Magnetic hyperthermia therapy: Magnetic hyperthermia, grounded on magnetic NPs having external alternating magnetic fields, is applied to transform magnetic energy into thermal energy for killing cancerous cells as tumor therapy generally (Fortin *et al*., 2007). The composite $La_{0.75}Sr_{0.25}MnO_3$ NPs have exhibited their high magnetic heat properties to treat diseased cells (Chen *et al*., 2017). The composite γ-$Mn_xFe_{2-x}O_3$ NPs ($0 \leq x \leq 1.3$) have been used to serve as magnetic hyperthermia agents for killing HeLa cells (Prasad *et al*., 2007), while magnetic NPs-mediated hyperthermia can induce antitumor immunity (Haghniasz *et al*., 2016).

Starvation therapy: Starvation therapy is applied to interrupt energy and nutrients supply to tumor cells for inducing metabolic disorders through lacking vast energy and nutrients supply to tumor cells required for their survival and growth compared to normal cells (Zhang *et al*., 2018). Glucose oxidase (GOx)-loaded MnO_2 NPs have been used for starvation therapy through a cascade reaction for disrupting the glucose metabolism and suppressing the ATP production (Yang *et al*., 2019; Pan *et al*., 2019). MnO_2-GOx-hyaluronic acid nanocomposites have been utilized to achieve O_2-promoted starvation therapy, while GOx may catalyze the oxidation of glucose into gluconic acid and H_2O_2 with O_2 consumption and MnO_2 may produce O_2 to support the process of glucose-depletion through reaction with H_2O_2 (Zhang *et al*., 2018a). Moreover, MnO_2 NMs have also been used for cancer starvation therapy through catalyzing glucose and O_2 into gluconic acid and H_2O_2 by their intrinsic GOx-like activity (Tang *et al*., 2019; Fu *et al*., 2018).

Photodynamic therapy: Though GSH overproduction and hypoxia within solid tumors restrict PDT efficiency owing to the O_2^- dependent therapeutic motif and potential GSH-scavenging effect on ROS, manganese oxide NPs can overcome these obstacles effectively by enhancing O_2 production and / or GSH depletion resulting reverse tumor hypoxia (Ding *et al*., 2019; Ding *et al*. 2019a; Gu *et al*., 2018). MnO doped carbon dots (CDs) NMs as O_2-self-sufficient PDT, have been used not only to produce $^1O_2$ but also to increase O_2 concentration by catalyzing H_2O_2 (Jia *et al*., 2018). Ce6-loaded MnO_2 NMs have been utilized as nanosystem through their disintegrated MnO_2 reduction by intracellular GSH and Ce6-release for fluorescence imaging with GSH-decrease for enhanced PDT (Fan *et al*., 2016). DOX-loaded UCNPs@$mSiO_2$-Ce6@MnO_2-PEG nanocomposites have also been used as tri-modal image-driven TME-self-enhanced chemodynamic therapy while MnO_2 is decomposed to produce O_2 and exhaust GSH and photosensitizer Ce6 activated by NIR light is penetrated deeply into the tissue owing to the introduction of UCNPs within solid tumors (Xu *et al*., 2018).

Chemodynamic therapy: Chemodynamic therapy (CDT) indicates the disproportionation of H_2O_2 via intratumoral Fenton-like of Fenton reactions for generating cytotoxic $^{\cdot}OH$ to induct cancer cell death through damaging biomolecules e.g. DNA, proteins and lipids (Lin *et al*., 2019; Ma *et al*., 2019). $mSiO_2$-DOX-MnO_2 NPs and few other MnO NPs exhibited their efficiencies as chemotherapy and GSH depletion-enhanced CDT producing cytotoxic $^{\cdot}OH$ for inducing cancer cell death (Lin *et al*., 2018; Ding *et al*., 2019; Zhen *et al*., 2019; Zhou *et al*., 2018). MnO_2@PtCo NPs showed their efficacies to catalyze cascades of intracellular biochemical reactions for producing free radicals through oxygen-sensitization in tumor therapy (Wang *et al*., 2018).

Sonodynamic therapy: Sonodynamic therapy (SDT) employs sonosensitizers to generate ROS by the application of ultrasound for cancer therapy to get high tumor-penetration depth with higher therapeutic efficiencies owing to its O_2-dependent potent GSH-scavenging effect on ROS (Chen *et al*., 2017). Protoporphyrin-loaded hollow organosilica NPs (HMONs)-MnOx (PMR) nanosonosensitizers showed higher cell killing efficacies for their GSH-exhausting and enhanced O_2-self-sifficient characteristics (Zhu *et al*., 2018).

Photothermal therapy: Photothermal therapy (PTT) employs the super-sensitive inorganic photothermal agent for high intrinsic photothermal heat conversion in biomedical applications (Schrantz *et al*., 1999). The stripped ultra-thin 2D MnO_2 nanosheets possessing the photothermal conversion ability showed their efficiencies against cancer (Liu *et al*., 2018a; Wang *et al*., 2019).

Radiotherapy: Radio therapy (RT) utilizes ionizing radiation from an internally placed radiation source or external beam to induct cellular damage through generation of free radicals, while MnO NPs showed to enhance RT to overcome tumor hypoxia owing to their O_2-generating capabilities (Ngwa *et al*., 2018; Juzenas *et al*., 2008; Hainfeld *et al*., 2008; Abbasi *et al*., 2016; Tao *et al*., 2018). Au@MnO_2 NPs and Au@MnO_2-PEG with X-ray irradiation exhibited enhanced tumor oxygenation to damage DNA for tumor inhibition (Yi *et al*., 2016). MnO_2 NPs encapsulated with HIF-1 inhibitor acriflavine (ACF) (ACF@MnO_2) showed enhanced RT via tumor oxygenation, functional HIF-1 and metastasis inhibitions (Meng *et al*., 2018). Additionally, ACF@MnO_2-PD-L1(checkpoint inhibitor antibody) exhibited its enhanced capabilities for activating tumor-specific immune responses such as productions of IFN-γ and $CD8^+$ T cells to inhibit tumorigenesis.

Combination therapy: Owing to a lot of challenges for tumor therapy such as high rate of recurrence, metastasis, individual variation and low survival, few MnO NPs-based combined therapeutic treatments showed their significant efficacies (Yu *et al*., 2018a; Fu *et al*., 2019; Fan *et al*., 2017). DOX-loaded MnO_2-coated black phosphorous nanosheet materials (BPN/MnO_2/DOX) exhibited their synergistic efficient supremacy for MRI-guided PDT, PTT and chemotherapy (Wu *et al*., 2019).

Toxicity: MnO NPs and their composite forms exhibited high cell viability as well as low cytotoxicity and good biocompatibility at a certain concentration. However, they showed significant cytotoxicity to tumor cells under certain doses through H_2O_2/GSH-dependent Fenton-like reaction compared to low level-H_2O_2/GSH contents and low cytotoxicity of normal cells (Lin *et al*., 2018; Ding *et al*., 2019; Zhou *et al*., 2018; Feng *et al*., 2018; Zhu *et al*., 2018). The doses higher than 93 mg/kg and 38 mg/kg for respective rats and mice caused toxicities, while Mn(II)-cations may be released from the acidic endosomal / lysosomal decomposition of the metabolized complex to accumulate into the liver,

pancreas and cardiac muscles causing hyperintensities and neurodegenerative disorders (Dobson *et al*., 2004; Racette *et al*., 2005; Silva *et al*., 2004; Aoki *et al*., 2004; Lee *et al*., 2005). DOX-loaded hollow manganese phosphate nanoparticles conjugated with folic acid (HMP-FA-DOX NPs) showed their folate receptor specific cytotoxic efficacies on tumor cells-killing through acidic endolysosomal releases of Mn^{2+} and DOX (Yu *et al*., 2012). Biodistribution and clearance: The biodistribution patterns of various ligand-coated manganese nanomaterials may vary by their different administrative routes. PEG-phospholipid / silica coated MnO NPs showed their highest accumulations in the liver after 24 / 4 h post-injections depending on the thickness of the coating materials to increase the blood half-life as well as hydrodynamic diameter beyond the renal filtration threshold (Howell *et al*., 2013; Hu *et al*., 2013; Yang *et al*., 2014; Mandal, 2018a). MnO NPs (6-8 nm) grafted with PEGylated bis-phosphonate dendrons exhibited their accumulations primarily in the faeces, intestine, gall bladder, kidneys and stomach in decreasing order relating their relatively negligible uptake by the mononuclear phagocyte system and their elimination over 70% of the injected dose from the body within 48 h (Chevallier *et al*., 2014). 4 h post intravenous injection of MnO NPs in mice showed preferential fluorescence accumulations to kidney, liver, lung and spleen, and lower accumulations in heart and brain, whereas no detection after 24 h indicating complete elimination from the body (Zheng *et al*., 2018).

Conclusion and future perspectives

Infectious, cancerous and other diseases suffer from drug toxicity and insolubility, non- selectivity and drug resistance. Metallic Mn NMs have been utilized to overcome these barriers in some extent as they possess good cellular biocompatibility and suitable physico-chemical characteristics. To minimize the side effects and to get significant biological efficacies, few Mn NPs have been synthesized with ligand-specific surface functionalities and coating to target specific cells with controlled cargo-release. However, further long term-exposed investigations are needed to get maximum *in vivo* targeting efficiencies of the ligand-anchored cargo-loaded Mn NMs with optimum formulation, dose, biocompatibility, biodistribution, pharmacokinetics, biodegradability, elimination, toxicity and administrative routes before going to their nanobiomedicinal translations into clinics.

Acknowledgements

This study was supported by the Council of Scientific and Industrial Research (CSIR),Government of India.

Conflict of interest: The authors declare no conflict of interest, financial or otherwise.

REFERENCES

Abbasi A.Z., Gordijo C.R., Amini M.A., Maeda A., Rauth A.M., Dacosta R.S. and Wu X.Y. 2016. Hybrid manganese dioxide nanoparticles potentiate radiation therapy by modulating tumor hypoxia. Cancer Res. 76: 6643-6656.

Aderibigbe B.A. 2017. Metal-based nanoparticles for the treatment of infectious diseases. Molecules 22: 1370.

Aoki I., Wu Y.J., Silva A.C., Lynch R.M. and Koretsky A.P. 2004. *In vivo* detection of neuroarchitecture in the rodent brain using manganese-enhanced MRI. Neuro-image 22: 1046-1059.

Apperlot G., Lipovsky A., Dror R., Perkas N., Nitzan Y., Lubart R. and Gedanken A. 2009. Enhanced antibacterial activity of nanocrystalline ZnO due to increased ROS-mediated cell injury. Adv. Funct. Mater. 19(6): 842-852.

Avila D.S., Puntel R.L. and Aschner M. 2013. Manganese in health and disease. Met. Ions Life Sci. 13: 199-227.

Bae K.H., Lee K., Kim C. and Park T.G. 2011. Surface functionalized hollow manganese oxide nanoparticles for cancer targeted siRNA delivery and magnetic resonance imaging. Biomater. 32: 176-184.

Baker C., Pradhan A., Pakstis L., Pocchan D.J. and Shah S.I. 2005. Synthesis and antibacterial properties of silver nanoparticles. J. Nanosci. Nanotechnol. 5: 244-249.

Born P.J., Robbins D., Haubold S., Kuhlbusch T., Fissan H., Donaldson K., Schins R., Stone V., Kreyling W., Lademann J., Krutmann J., Warheit D. and Oberdorster E. 2006. The potential risks of nanomaterials: a review carried out for ECETOC. Particle Fibre Toxicol. 3(1): 11.

Brown J.M. 2007. Tumor hypoxia in cancer therapy. Methods Enzymol. 435: 297-321.

Bump E.A. and Brown J.M. 1990. Role of glutathione in the radiation response of mammaliancells *in vitro* and *in vivo*. Pharmacol. Ther. 47: 117-136.

Chen J., Luo H., Liu Y., Zhang W., Li H., Luo T., Zhang K., Zhao Y. and Liu J. 2017. Oxygen-self-produced nanoplatform for relieving hypoxia and breaking resistance to sonodynamic treatment of pancreatic cancer. ACS. Nano 11(12): 12849-12862.

Chen J.L., Li L., Wang S., Sun X.Y., Xiao L., Ren J.S., Di B. and Gu N. 2017a. A glucose-activatable trimodal glucometer self-assembled from glucose oxidase and MnO_2 nanosheets for diabetes monitoring. J. Mater. Chem. B. 5: 5336-5344.

Chen Y., Ye D., Wu M., Chen H., Zhang L., Shi J. and Wang L. 2014. Break-up of two-dimensional MnO_2 nanosheets promotes ultrasensitive pH-triggered theranostics of cancer. Adv. Mater. 26(41): 7019-7026.

Cherian E., Rajan A. and Baskar G. 2016. Synthesis of manganese dioxide nanoparticles using co-precipitation method and its antimicrobial activity. Int. J. Modern Sci. Technol. 1: 17-22.

Chevallier P., Walter A., Garofalo A., Veksler I., Lagueux J., Begin-Colin S., Felder-Flesch D. and Fortin M.A. 2014. Tailored biological retention and efficient clearance of pegylated ultra-small MnO nanoparticles as positive MRI contrast agents for molecular imaging. J. Mater. Chem. B. 2: 1779-1790.

Cho M.H., Choi E.S., Kim S., Goh S.H. and Choi Y. 2017. Redox-responsive manganese dioxide nanoparticles for enhanced MR imaging and radiotherapy of lung cancer. Front. Chem. 5: 109.

Chu H., Zhao J., Mi Y., Di Z. and Li L. 2019. NIR-light-mediated spatially selective triggering of anti-tumor immunity via upconversion nanoparticle-based immunodevices. Nat. Commun. 10: 2839.

Dai Y., Xu C., Sun X. and Chen X. 2017. Nanoparticle design strategies for enhanced anticancer therapy by exploiting the tumor microenvironment. Chem. Soc. Rev. 46: 3830.

DeJong W.H. and Borm, P.J.A. 2008. Drug delivery and nanoparticles: applications and hazards. Int. J. Nanomed. 3: 133-149.

Deng B., Shao S., Yu C., Teng B., Wang M., Cheng Z., Wong K.L., Ma P.A. and Lin J. 2018. Large-pore mesoporous-silica-coated upconversion nanoparticles as multifunctional immunoadjuvants with ultra high photosensitizer and antigen loading efficiencyfor improved cancer photodynamic immunotherapy. Adv. Mater. 30(52): e1802479.

Ding B., Shao S., Jiang F., Dang P., Sun C., Huang S., Ma P.A., Jin D., Al Kheraif A.A. and Lin J. 2019. MnO_2-disguised upconversion hybrid nanocomposite: an ideal architecture for tumor microenvironment-triggered UCL / MR bioimaging and enhanced chemodynamic therapy. Chem. Mater. 31(7): 2651-2660.

Ding B., Shao S., Xiao H., Sun C., Cai X., Jiang F., Zhao X., Ma P.A. and Lin J. 2019a. $MnFe_2O_4$-decorated large-pore mesoporous silica-coated upconversion nanoparticles for near-infrared light-induced and O_2 self-sufficient photodynamic therapy. Nanoscale 11(31): 14654-14667.

Dizaj S.M., Loftifur F., Jalali M.B., Jarrintan M.H. and Adibkia K. 2014. Anti-microbial activity of the metals and metal oxide nanoparticles. Mater. Sci. Eng. C. 44: 278-284.

Dobson A.W., Erikson K.M. and Aschner M. 2004. Manganese neurotoxicity. Ann. N.Y. Acad. Sci. 1012: 115-128.

Du B., Ding X., Wang H., Du Q., Xu T., Huang J., Zhou J. and Cheng G. 2019. Development of an interactive tumor vascular suppression strategy to inhibit multidrug resistance and metastasis with pH/H_2O_2-responsive and oxygen-producing nanohybrids. J. Mater. Chem. B. 7: 4784.

Dunbar C.E., High K.A., Joung J.K., Kohn D.B., Ozawa K. and Sadelain M. 2018. Gene therapy comes of age. Sci. 359(6372): 175.

Facciabene A., Peng X., Hagemann I.S., Balint K., Barchetti A., Wang L.P., Gimotty P.A., Gilks C.B., Lal P., Zhang L. and Coukos G. 2011. Tumor hypoxia promotes tolerance and angiogenesis via CCL28 and T (reg) cells. Nature 475(7355): 226-230.

Fan H., Yan G., Zhao Z., Hu X., Zhang W., Liu H., Fu X., Fu T., Zhang X.B. and Tan W. 2016. A smart photosensitizer-manganese dioxide nanosystem for enhanced photodynamic therapy by reducing glutathione levels in cancer cells. Angew. Chem. Int. Ed. Engl. 55(18): 5477-5482.

Fan H., Zhao Z., Yan G., Zhang X., Yang C., Meng H., Chen Z., Liu H. and Tan W. 2015. A smart DNAzyme-MnO_2 nanosystem for efficient gene silencing. Angew. Chem. Int. Ed. Engl. 54(16): 4801-4805.

Fan W., Yung B., Huang P. and Chen X. 2017. Nanotechnology for multimodal synergistic cancer therapy. Chem. Rev. 117(22): 13566-13638.

Feng L.L., Xie R., Wang C.Q., Gai S.L., He F., Yang D., Yang P.P. and Lin J. 2018. Magnetic targeting, tumor microenvironment-responsive intelligent nanocatalysts for enhanced tumor ablation. ACS. Nano 12(11): 11000-11012.

Fortin J.P., Wilhelm C., Servais J., Menager C., Bacri J.C. and Gazeau F. 2007. Size-sorted anionic iron oxide nanomagnets as colloidal mediators for magnetic hyperthermia. J. Am. Chem. Soc. 129(9): 2628-2635.

Fu L.H., Qi C., Hu Y.R., Lin J. and Huang P. 2019. Glucose oxidase-instructed multimodal synergistic cancer therapy. Adv. Mater. 31(21): 1808325.

Fu L.H., Qi C., Lin J. and Huang P. 2018. Catalytic chemistry of glucose oxidase in cancer diagnosis and treatment. Chem. Soc. Rev. 47: 6454-6472.

Gao S., Wang G., Qin Z., Wang X., Zhao G., Ma Q. and Zhu L. 2017. Oxygen generating hybrid nanoparticles to enhance fluorescent / photoacoustic / ultrasound imaging guided tumor photodynamic therapy. Biomater. 112: 324-335.

Gopalakrishnan V., Spencer C.N., Nezi L., Reuben A., Andrews M.C., Karpinets T.V., Prieto P.A., Vicente D., Hoffman K., Wei S.C., Cogdill A.P., Zhao L., Hudgens C.W., Hutchinson D.S., Manzo T., deMacedo M.P., Cotechini T., Kumar T., Chen W.S., Reddy S.M., Sloane R.S., Galloway-Pena J., Jiang H., Chen P.L., Shpall E.J., Rezvani K., Alousi A.M., Chemaly R.F., Shelburne S., Vence L.M., Okhuysen P.C., Jensen V.B., Swennes A.G., McAllister F., Sanchez E.M.R., Zhang Y., Chatelier E.L., Zitvogel L., Pons N., Austin-Breneman J.L., Haydu L.E., Burton E.M., Gardner J.M., Sirmans E., Hu J., Lazar A.J., Tsujikawa T., Diab A., Tawbi H., Glitza I.C., Hwu W.J., Patel S.P., Woodman S.E., Amaria R.N., Davies M.A., Gershenwald J.E., Hwu P., Lee J.E., Zhang J., Coussens L.M., Cooper Z.A., Futreal P.A., Daniel C.R., Ajami N.J., Petrosino J.F., Tetzlaff M.T., Sharma P., Allison J.P., Jenq R.R. and Wargo J.A. 2018. Gut microbiome modulates response to anti-PD-1 immunotherapy in melanoma patients. Sci. 359(6371): 97-103.

Greish K. 2010. Cancer nanotechnology: methods and protocols (eds Grobmyer SR, Moudgil BM) (Humana Press, New York), pp. 25-37.

Gu T., Cheng L., Gong F., Xu J., Li X., Han G. and Liu Z. 2018. Upconversion composite nanoparticles for tumor hypoxia modulation and enhanced near-infrared-triggered photodynamic therapy. ACS. Appl. Mater. Interf. 10(18): 15494-15503.

Guo M., Que C., Wang C., Liu X., Yan H. and Liu K. 2011. Multifunctional superparamagnetic nanocarriers with folate-mediated and pH-responsive targeting properties for anticancer drug delivery. Biomater. 32: 185-194.

Haghniasz R., Umrani R.D. and Paknikar, K.M. 2016. Hyperthermia mediated by dextran-coated $La_{0.7}Sr_{0.3}MnO_3$ nanoparticles: *in vivo* studies. Int. J. Nanomed. 11: 1779.

Hainfeld J.F., Dilmanian F.A., Slatkin D.N. and Smilowitz H.M. 2008. Radiotherapy enhancement with gold nanoparticles. J. Pharm. Pharmacol. 60(8): 977-985.

Hajipur M.J., Fromm K.M., Ashkarran A.A., deAbrasturi D.J., deLarramendi I.R. and Rojo T. 2012. Antibacterial properties of nanoparticles. Trends Biotechnol. 30: 499-511.

Haneefa M.M., Jayandran M. and Balasubramanian V. 2017. Green synthesis, characterization and antimicrobial activity evaluation of manganese oxide nanoparticles and comparative studies with salicylalchitosan functionalized nanoform. Asian J. Pharmaceut. 11(1): 65-74.

Haneefa M.M., Jayandran M. and Balasubramanian V. 2017a. Evaluation of antimicrobial activity of green-synthesized manganese oxide nanoparticles and comparative studies with curcuminaniline functionalized nanoform. Asian J. Pharm. Clin. Res. 10(3): 347-352.

Hao X.L., Zhao J.Z., Zhao Y., Ma D.C., Lu Y., Guo J.N. and Zeng Q. 2013. Mild aqueous synthesis of urchin-like MnOx hollow nanostructures and their properties for RhB degradarion. Chem. Eng. J. 229: 134-143.

He D., He X., Wang K., Yang X., Yang X., Zou Z. and Li X. 2015. Redox-responsive degradable honeycomb

manganese oxide nanostructures as effective nanocarriers for intracellular glutathione-triggered drug release. Chem. Commun. 51: 776.

Hoseinpour V. and Ghaemi N. 2018. Novel ZnO-MnO_2-Cu_2O triple nanocomposite: facial synthesis, characterization, antibacterial activity and visible light photocatalytic performance for dyes degradation - a comparative study. Mat. Res. Express. 5: 85012.

Howell M., Mallela J., Wang C., Ravi S., Dixit S., Ganapati U. and Mohapatra S. 2013. Manganese-loaded lipid-micellar theranostics for simultaneous drug and gene delivery to lungs. J. Control. Rel. 167(2): 210-218.

Hu H., Dai A., Sun J., Li X., Gao F., Wu L., Fang Y., Yang H., An L., Wu H. and Yang S. 2013. Aptamer-conjugated Mn_3O_4@SiO_2 core-shell nanoprobes for targeted magnetic resonance imaging. Nanoscale 5: 10447-10454.

Jalal R., Goharshadi E.K., Abareshi M., Moosavi M., Yousefi A. and Nancarrow P. 2010. ZnO nanofluids: green synthesis, characterization, and antibacterial activity. Mater. Chem. Phys. 121: 198-201.

Jayandran M., Haneefa M.M. and Balasubramanian V. 2015. Green synthesis and characterization of manganese nanoparticles using natural plant extracts and its evaluation of antimicrobial activity. J. Appl. Pharmaceut. Sci. 5(12): 105-110.

Jia Q., Ge J., Liu W., Zheng X., Chen S., Wen Y., Zhang H. and Wang P. 2018. A magneto fluorescent carbon dot assembly as an acidic H_2O_2-driven oxygenator to regulate tumor hypoxia for simultaneous bimodal imaging and enhanced photodynamic therapy. Adv. Mater. 30(13): e1706090.

Juzenas P., Chen W., Sun Y.P., Netocoelho M.A., Generalov R., Generalova N. and Christensen I.L. 2008. Quantum dots and nanoparticles for photodynamic and radiation therapies of cancer. Adv. Drug Deliv. Rev. 60(15): 1600-1614.

Koo H., Huh M.S., Sun I.C., Yuk S.H., Choi K., Kim K. and Kwon I.C. 2011. *In vivo* targeted delivery of nanoparticles for theranosis. Acc. Chem. Res. 44: 1018-1028.

Krolikowska A., Kudelski A., Michota A. and Bukowska J. 2003. SERS studies on the structure of thioglycolic acid monolayers on silver and gold. Surf. Sci. 532: 227-232.

Lee J.H., Silva A.C., Merkle H. and Koretsky A.P. 2005. Manganese-enhanced magnetic resonance imaging of mouse brain after systemic administration of $MnCl_2$: Dose dependent and temporal evolution of T1 contrast. Magn. Reson. Med. 53: 640-648.

Li C., Liu H., Sun Y., Wang H., Guo F., Rao S., Deng J., Zhang Y., Miao Y., Guo C., Meng J., Chen X., Li L., Li D., Xu H., Wang H., Li B. and Jiang C. 2009. PAMAM nanoparticles promote acute lung injury by inducing autophagic cell death through the Akt-TSC_2-mTOR signaling pathway. J. Mol. Cell. Biol. 1(1): 37-45.

Liang R., Liu L., He H., Chen Z., Han Z., Luo Z., Wu Z., Zhang M., Ma Y. and Cai L. 2018. Oxygen-boosted immunogenic photodynamic therapy with gold nanocages@manganese dioxide to inhibit tumor growth and metastases. Biomater. 177: 149-160.

Lin L.S., Huang T., Song J., Ou X.Y., Wang Z., Deng H., Tian R., Liu Y., Wang J.F., Liu Y., Yu G., Zhou Z., Wang S., Niu G., Yang H.H. and Chen X. 2019. Synthesis of coper peroxide nanodots for H_2O_2 self-supplying chemodynamic therapy. J. Am. Chem. Soc. 141: 9937-9945.

Lin L.S., Song J., Song L., Ke K., Liu Y., Zhou Z., Shen Z., Li J., Yang Z., Tang W., Niu G., Yang H.H. and Chen X. 2018. Simultaneous Fenton-like ion delivery and glutathione depletion by MnO_2-based nano agent to enhance chemodynamic therapy. Angew. Chem. Int. Ed. Engl. 57(18): 4902-4906.

Liu J., Chen Q., Feng L. and Liu Z. 2018. Nanomedicine for tumor microenvironment modulation and cancer treatment enhancement. Nano Today 21:55.

Liu Z., Zhang S., Lin H., Zhao M., Yao H., Zhang L., Peng W. and Chen Y. 2018a. Theranostic 2D ultrathin MnO_2 nanosheets with fast responsibility to endogenous tumor microenvironment and exogenous NIR irradiation. Biomater. 155: 54-63.

Lu Y., Zhang L., Li J., Su Y.D., Liu Y., Xu Y.J., Dong L., Gao H.L., Lin J., Man N., Wei P.F., Xu W.P., Yu S.H. and Wen L.P. 2013. MnO nanocrystals: a platform for integration of MRI and genuine autophagy induction for chemotherapy. Adv. Funct. Mater. 23(12): 1534-1546.

Ma B., Wang S., Liu F., Zhang S., Duan J., Li Z., Kong Y., Sang Y., Liu H., Bu W. and Li L. 2019. Self-assembled copper-amino acid nanoparticles for in situ glutathione and H_2O_2 sequentially triggered chemodynamic therapy. J. Am. Chem. Soc. 141(2): 849-857.

Maeda H., Wu J., Sawa T., Matsumura Y. and Hori K. 2000. Tumor vascular permeability and the EPR effect in macromolecular therapeutics: a review. J. Control. Rel. 65: 271-284.

Mandal A.K. 2017. Silver nanoparticles as drug delivery vehicle against infections. Glob. J. Nanomed. 3(2): 555607.

Mandal A.K. 2017a. Copper nanomaterials as drug delivery system against infectious agents and cancerous cells. J. Appl. Life Sci. Int. 15(4): 38444.

Mandal A.K. 2018. Gold nanoparticles as delivery system against diseases. Lativa, European Union: LAP LAMBERT Academic Publishing (SIA OmniScriptum Publishing), p. 1-45.

Mandal A.K. 2018a. Zinc oxide nanoparticles as delivery system to combat diseases. Int. J. Curr. Adv. Res. 7(5D): 12469-12478.

Mandal A.K. 2019. Titanium dioxide nanoparticles as delivery system against infections and cancer. Int. J. Curr. Res. 11(1): 68-72.

Mandal A.K. 2021. Dendrimers in targeted drug delivery applications: A review of diseases and cancer. Int. J. Polym. Mater. Polym. Biomater. 70(4): 287-297.

Mandal A.K., Ghosh D., Sarkar S., Ghosh A., Swarnakar S. and Das N. 2014. Nanocapsulated quercetin downregulates rat hepatic MMP-13 and controls diethylnitrosamine-induced carcinoma. Nanomed (Lond). 9(15): 2323-2337.

McCarthy J.R. and Weissleder R. 2008. Multifunctional magnetic nanoparticles for targeted imaging and therapy. Adv. Drug Deliv. Rev. 60: 1241-1251.

Meng H., Liong M., Xia T., Li Z., Ji Z., Zink J.I. and Nel A.E. 2010. Engineered design of mesoporous silica nanoparticles to deliver doxorubicin and P-glycoprotein siRNA to overcome drug resistance in a cancer cell line. ACS. Nano. 4(8): 4539-4550.

Meng L., Cheng Y., Tong X., Gan S., Ding Y., Zhang Y., Wang C., Xu L., Zhu Y., Wu J., Hu Y. and Yuan A. 2018. Tumor oxygenation and hypoxia inducible factor-1 functional inhibition via a reactive oxygen species

responsive nanoplatform for enhancing radiation therapy and abscopal effects. ACS. Nano 12(8): 8308-8322.

Mody V.V., Siwale R., Singh A. and Mody H.R. 2010. Introduction to metallic nanoparticles. J. Pharm. Bioall. Sci. 2: 282-289.

Muz B., de la Puente P., Azab F. and Azab A.K. 2015. The role of hypoxia in cancer progression, angiogenesis, metastasis, and resistance to therapy. *Hypoxia* (Auckl.). 3: 83-92.

Na H.B., Lee J.H., An K., Park Y., Park M., Lee I.S., Nam D.H., Kim S.T., Kim S.H., Kim S.W., Lim K.H., Kim K.S., Kim S.O. and Hyeon T. 2007. Development of a T1 contrast agent for magnetic resonance imaging using MnO nanoparticles. Angew. Chem. Int. Ed. Engl. 46: 5397-5401.

National Institutes of Health (US). 2007. Biological sciences curriculum study NIH curriculum supplement series. In understanding emerging and re-emerging infectious diseases; National Institutes of Health (US): Bethesda, MD, USA. https://www.ncbi.nlm.nih.gov/books/NBK20370/ (accessed on 20 April 2017)

Ngwa W., Irabor O.C., Schoenfeld J.D., Hesser J., Demaria S., Formenti S.C. 2018. Using immunotherapy to boost the abscopal effect. Nat. Rev. Cancer 18(5): 313-322.

Ogunyemi S.O., Zhang F., Abdallah Y., Zhang M., Wang Y., Sun G., Qiu W. and Li B. 2019. Biosynthesis and characterization of magnesium oxide and manganese dioxide nanoparticles using *Mtricaria chamomilla* L. extract and its inhibitory effect on *Acidovorax oryzae* strain RS-2. Artif. cells Nanomed. Biotechnol. 47(1): 2230-2239.

Pan W., Ge Y., Yu Z., Zhou P., Cui B., Li N., Tang B. 2019. A cancer cell membrane-encapsulated MnO_2 nanoreactor for combined photodynamic-starvation therapy. Chem. Commun. 55: 5115-5118.

Pardoll D.M. 2012. The blockade of immune checkpoints in cancer immunotherapy. Nat. Rev. Cancer 12(4): 252-264.

Prasad N.K., Rathinasamy K., Panda D. and Bahadur D. 2007. Mechanism of cell death induced by magnetic hyperthermia with nanoparticles of γ-$Mn_xFe_{2-x}O_3$ synthesized by a single step process. J. Mater. Chem. 17: 5042-5051.

Racette B.A., Antenor J.A., McGee-Minnich L., Moerlein S.M., Videen T.O., Kotagal V. and Perlmutter J.S. 2005. [18F]FDOPA PET and clinical features in parkinosonism due to manganism. Mov. Disorder 20, 492-496.

Rapisarda A. and Melillo G. 2010. "Combination strategies targeting hypoxic inducible factor (HIF-1) for cancer therapy", in The Tumor Microenvironment, ed Bagley R (New York, NY:Springer): 3-21.

Ren S., Yang J., Ma L., Li X., Wu W., Liu C., He J. and Miao L. 2018. Ternary-responsive drug delivery with activatable dual mode contrast-enhanced *in vivo* imaging. ACS. Appl. Mater. Interf. 10(38): 31947-31958.

Sana S., Ghosh S., Das N., Sarkar S. and Mandal A.K. 2017. Vesicular melatonin efficiently downregulates sodium fluoride-induced rat hepato- and broncho- TNF-α, TGF-β expressions, and associated oxidative injury: a comparative study of liposomal and nanoencapsulated forms. Int. J. Nanomed. 12: 4059-4071.

Schrantz N., Blanchard D.A., Mitenne F., Auffredou M.T., Vazquez A. and Leca G. 1999. Manganese induces apoptosis of human B cells: caspase-dependent cell death blocked by bcl-2. Cell death Differ. 6: 445-453.

Shankar B., Krishnan S., Vasantha M., Arun B. and Williams P.H. 2009. Outer membrane proteins of wild-type and intimin-deficient enteropathogenic *Eschericia coli* induce Hep-2 cell death through intrinsic and extrinsic pathways of apoptosis. Int. J. Med. Microbiol. 299: 121-132.

Shin J., Anisur R.M., Ko M.K., Im G.H., Lee J.H. and Lee I.S. 2009. Hollow manganese oxide nanoparticles as multifunctional agents for magnetic resonance imaging and drug delivery. Angew. Chem. Int. Ed. Engl. 48: 321-324.

Silva A.C., Lee J.H., Aoki I. and Koretsky A.P. 2004. Manganese-enhanced magnetic resonance imaging (MEMRI): Methodological and practical considerations. NMR. Biomed. 17: 532-543.

Singh M., Manikandan S. and Kumaraguru A.K. 2011. Nanoparticles: a new technology with wide applications. Res. J. Nanosci. Nanotechnol. 1: 1-11.

Sirelkhalim A., Mahmud S., Seeni A., Kaus N.H.M., Ann L.C. and Bakhori S.K.M. 2015. Review on zinc oxide nanoparticles: antibacterial activity and toxicity mechanism. Nano Micro Lett. 7: 219-242.

Sudimack J. and Lee R.J. 2000. Targeted drug delivery via the folate receptor. Adv. Drug Deliv. Rev. 41: 147-162.

Tang W., Fan W., Zhang W., Yang Z., Li L., Wang Z., Chiang Y.L., Liu Y., Deng L., He L., Shen Z., Jacobson O., Aronova M.A., Jin A., Xie J. and Chen X. 2019. Wet / sono-chemical synthesis of enzymatic two-dimensional MnO_2 nanosheets for synergistic catalysis-enhanced photo theranostics. Adv. Mater. 31(19): 1900401.

Tao Y., Zhu L., Zhao Y., Yi X., Zhu L., Ge F., Mou X., Chen L., Sun L. and Yang K. 2018. Nano-graphene oxide-manganese dioxide nanocomposites for overcoming tumor hypoxia and enhancing cancer radioisotope therapy. Nanoscale 10(11): 5114-5123.

Teicher B.A. 1995. Physiologic mechanisms of therapeutic resistance. Blood flow and hypoxia. Hematol. Oncol. Clin. North. Am. 9: 475-506.

Thomas H., Coley H.M. 2003. Overcoming multidrug resistance in cancer: an update on the clinical strategy of inhibiting P-glycoprotein. Cancer Control. 10(2): 159-165.

Vaupel P. and Mayer A. 2007. Hypoxia in cancer: significance and impact on clinical outcome. Cancer Metastasis Rev. 26: 225-239.

Wang L., Guan S.Y., Weng Y.Z.W., Xu S.M., Lu H., Meng X.M. and Zhou S.Y. 2019. Highly efficient vacancy-driven photothermal therapy mediated by ultrathin MnO_2 nanosheets. ACS. Appl. Mater. Interf. 11: 6267-6275.

Wang L.L., Hu C. and Shao L.Q. 2017. The antimicrobial activity of nanoparticles: present situation and prospects for the future. Int. J. Nanomed. 12: 1227-1249.

Wang X., Dai J., Wang X., Hu Q., Huang K., Zhao Z., Lou X. and Xia F. 2019a. MnO_2-DNAzyme-photosensitizer nanocomposite with AIE characteristic for cell imaging and photodynamic-gene therapy. Talanta. 202: 591-599.

Wang Z., Zhang Y., Ju E., Liu Z., Cao F., Chen Z., Ren J. and Qu X. 2018. Biomimetic nanoflowers by self-assembly of nanozymes to induce intracellular oxidative damage against hypoxic tumors. Nat. Commun. 9: 3334.

Wang Z., Zhang Y., Liu Z., Dong K., Liu C., Ran X., Pu F., Ju E., Ren J. and Qu X. 2017a. A bifunctional nanomodulator for boosting CpG-mediated cancer immunotherapy. Nanoscale. 9: 14236-14247.

Wu Q., Chen G., Gong K., Wang J., Ge X., Liu X., Guo S. and Wang F. 2019. MnO_2-laden black phosphorous for MRI-

guided synergistic PDT, PTT and chemotherapy. Matter. 1: 496-512.

Xu J., Han W., Yang P., Jia T., Dong S., Bi H., Gulzar A., Yang D., Gai S., He F., Lin J. and Li C. 2018. Tumor microenvironment-responsive mesoporous MnO_2-coated upconversion nanoplatform for self-enhanced tumor theranostics. Adv. Funct. Mater. 28(36): 1803804.

Xu J., Han W., Yang P., Jia T., Dong S., Bi H., Gulzar A., Yang D., Gai S., He F., Lin J. and Li C. 2018a. Tumor microenvironment-responsive mesoporous MnO_2-coated upconversion nanoplatform for self-enhanced tumor theranostics. Adv. Funct. Mater. 28(36): 1803804.

Yang G., Xu L., Chao Y., Xu J., Sun X., Wu Y., Peng R. and Liu Z. 2017. Hollow MnO_2 as a tumor-microenvironment-responsive biodegradable nano-platform for combination therapy favoring antitumor immune responses. Nat. Commun. 8: 902.

Yang X., Yang Y., Gao F., Wei J.J., Qian C.G. and Sun M.J. 2019. Biomimetic hybrid nanozymes with self-supplied H^+ and accelerated O_2 generation for enhanced starvation and photodynamic therapy against hypoxic tumors. Nano Lett. 19(7): 4334-4342.

Yang X., Zhou Z., Wang L., Tang C., Yang H. and Yang S. 2014. Folate conjugated Mn_3O_4@SiO_2 nanoparticles for targeted magnetic resonance imaging *in vivo*. Mater. Res. Bull. 57: 97-102.

Yi X., Chen L., Zhong X., Gao R., Qian Y., Wu F., Song G., Chai Z., Liu Z. and Yang K. 2016. Core-shell Au@MnO_2 nanoparticles for enhanced radiotherapy via improving the tumor oxygenation. Nano Res. 9: 3267-3278.

Yoo H.S. and Park T.G. 2004. Folate-receptor-targeted delivery of doxorubicin nano-aggregares stabilized by doxorubicin-PEG-folate conjugate. J. Control. Rel. 100: 247-256.

Yu C., Ding B., Zhang X., Deng X., Deng K., Cheng Z., Xing B., Jin D., Ma P.A. and Lin J. 2018. Targeted iron nanoparticles with platinum-(IV) prodrugs and anti-EZH_2 siRNA show great synergy in combating drug resistance *in vitro*. Biomater. 155: 112-123.

Yu J., Hao R., Sheng F., Xu L., Li G. and Hou Y. 2012. Hollow manganese phosphate nanoparticles as smart multifunctional probes for cancer cell targeted magnetic resonance imaging and drug delivery. Nano Res. 5(10): 679-694.

Yu L., Hu P. and Chen Y. 2018a. Gas-generating nanoplatforms: Material chemistry, multifunctionality, and gas therapy. Adv. Mater. 30(49):1801964.

Zhang M., Xing L., Ke H., He Y.J., Cui P.F., Zhu Y., Jiang G., Qiao J.B., Lu N., Chen H. and Jiang H.L. 2017. MnO_2-based nanoplatform serves as drug vehicle and MRI contrast agent for cancer theranostics. ACS. Appl. Mater. Interf. 9(13): 11337-11344.

Zhang R., Feng L., Dong Z., Wang L., Liang C., Chen J., Ma Q., Zhang R., Chen Q., Wang Y. and Liu Z. 2018. Glucose and oxygen exhausting liposomes for combined cancer starvation and hypoxia-activated therapy. Biomater. 162: 123-131.

Zhang Y., Kohler N. and Zhang M. 2002. Surface modification of superparamagnetic magnetite nanoparticles and their intracellular uptake. Biomater. 23: 1553-1561.

Zhang Y.H., Qiu W.X., Zhang M., Zhang L. and Zhang X.Z. 2018a. MnO_2 motor: a prospective cancer-starving therapy promoter. ACS. Appl. Mater. Interf. 10(17): 15030-15039.

Zhao G. and Stevens S.E. 1998. Multiple parameters for the comprehensive evaluation of the susceptibility of *Escherichia coli* to the silver ion. BioMetals 11: 27-32.

Zhao L., Ge X., Zhao H., Shi L., Capobianco J.A., Jin D. and Sun L. 2018. Double-sensitive drug release system based on MnO_2 assembled upconversion nanoconstruct for double-model guided chemotherapy. ACS. Appl. Nano Mater. 1(4): 1648-1656.

Zhao P., Zhu Y., Yang X., Shen J., Jiang X., Zong J. and Li C. 2014. Multifunctional MnO_2 nanosheet-modified Fe_3O_4@SiO_2/$NaYF_4$:Yb,Er nanocomposites as novel drug carriers. Dalton Trans. 43(2): 451-457.

Zhen W., Wang W., Ma Z., Bai J., Jia X., Ruan Y., Wang C., Zhang M. and Jiang X. 2019. Multienzyme-mimicking nanocomposite for tumor phototheranostics and normal cell protection. Chem. Nano Mat. 5: 101-109.

Zheng Y., Zhang H., Hu Y., Bai L. and Xue J. 2018. MnO nanoparticles with potential application in magnetic resonance imaging and drug delivery for myocardial infarction. Int. J. Nanomed. 13: 6177-6188.

Zhou L., Wu Y., Meng X., Li S., Zhang J., Gong P., Zhang P., Jiang T., Deng G., Li W., Sun Z. and Cai L. 2018. Dye-anchored MnO nanoparticles targeting tumor and inducing enhanced phototherapy effect via mitochondria-mediated pathway. Small. 14(36): e1801008.

Zhu P., Chen Y. and Shi J. 2018. Nanozyme-augmented cancer sonodynamic therapy by catalytic tumor oxygenation. ACS. Nano 12(4): 3780-3795.

Zhu W., Dong Z., Fu T., Liu J., Chen Q., Li Y., Zhu R., Xu L. and Liu Z. 2016. Modulation of hypoxia in solid tumor microenvironment with MnO_2 nanoparticles to enhance photodynamic therapy. Adv. Funct. Mater. 26(30): 5490-5498.

Zong X. and Wang L. 2014. Ion-exchangeable semiconductor materials for visible light-induced photocatalysis. J. Photochem. Photobiol. C: Photochem. Rev. 18: 32-49.

****